

MixFlow Training: Alleviating Exposure Bias with Slowed Interpolation Mixture

Hui Li¹ Jiayue Lyu¹ Fu-Yun Wang² Kaihui Cheng¹ Siyu Zhu^{1,4,5} Jingdong Wang³
¹Fudan University ²The Chinese University of Hong Kong ³Baidu
⁴Shanghai Innovation Institute ⁵Shanghai Academy of AI for Science

<https://mixflowgen.github.io/>

Abstract

This paper studies the training-testing discrepancy (a.k.a. exposure bias) problem for improving the diffusion models. During training, the input of a prediction network at one training timestep is the corresponding ground-truth noisy data that is an interpolation of the noise and the data, and during testing, the input is the generated noisy data. We present a novel training approach, named MixFlow, for improving the performance. Our approach is motivated by the Slow Flow phenomenon: the ground-truth interpolation that is the nearest to the generated noisy data at a given sampling timestep is observed to correspond to a higher-noise timestep (termed slowed timestep), i.e., the corresponding ground-truth timestep is slower than the sampling timestep. MixFlow leverages the interpolations at the slowed timesteps, named slowed interpolation mixture, for post-training the prediction network for each training timestep. Experiments over class-conditional image generation (including SiT, REPA, and RAE) and text-to-image generation validate the effectiveness of our approach. Our approach MixFlow over the RAE models achieve strong generation results on ImageNet: 1.43 FID (without guidance) and 1.10 (with guidance) at 256×256 , and 1.55 FID (without guidance) and 1.10 (with guidance) at 512×512 .

1. Introduction

We study the training-testing discrepancy problem [32, 36], also known as exposure bias [11, 20, 22, 27, 28], for diffusion and flow matching models. During training, diffusion models learn a prediction network, where the input to the prediction network at each training timestep is the corresponding *ground-truth* noisy data, i.e., an interpolation of the noise and the data. During testing, the input to the prediction network is the *generated* noisy data. The difference of the inputs to the prediction network for training and testing, i.e., the training-testing discrepancy, is one of the reasons leading to the prediction discrepancy and accordingly the problems of error accumulation and sampling drift.

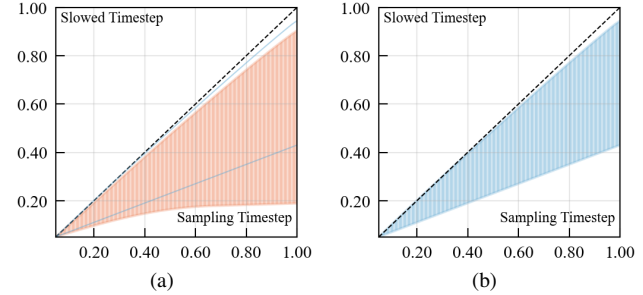


Figure 1. Illustrating (1) the *Slow Flow* phenomenon during the sampling process: the timestep (y-axis), corresponding to the ground truth noisy data that is the nearest to the generated noisy data at the sampling timestep t (x-axis), is slower (with higher noise), i.e., the shading area is under the line $x = y$; and (2) the effectiveness of MixFlow training: the range of slowed timesteps for (b) MixFlow training is smaller and closer to the sampling steps than (a) standard training, indicating that MixFlow training effectively alleviates the training-testing discrepancy. The boundary of the shading area in (b) is plotted as blue lines in (a). Note: x-axis - the sampling timestep at which the noisy data is generated; y-axis - the slowed timestep corresponding to the ground truth noisy data that is the nearest to the generated noisy data; shading area - the range (the vertical line) of slowed timesteps at each sampling step; noise corresponds to timestep 0, and data corresponds to timestep 1. The slowed timestep ranges are obtained from 20,000 training images in ImageNet [1], 50 sampling steps, and SiT-B [26]. Details on how to plot the figures are provided in Appendix A.

There are two main lines of solutions to alleviating the discrepancy problem. One line is to modify the training procedure [11, 27]. For example, Input Perturbation [27] conducts an input perturbation on the ground truth noisy data, and self-forcing [11] uses the generated noisy data as the input. The other line is to modify the sampling process [20, 28, 33, 53]. For example, Epsilon Scaling [28] scales the predicted noise during sampling, and Time-Shift Sampler [20] shifts the sampling timestep for the next sampling iteration. In this paper, we are interested in the former line and present a novel training procedure.

Our approach is motivated by the *Slow Flow* phe-

nomenon about the generated noisy data and its nearest ground-truth noisy data. Figure 1 illustrates the *Slow Flow* phenomenon. The nearest ground-truth noisy data to the generated noisy data at the sampling timestep t is observed to corresponds to a higher-noise timestep, called *Slowed Timestep* m_t . This intuitively means that the generated noisy data is slower than the ground truth noise data, i.e., the higher-noise timestep slower than the sampling timestep ($m_t \leq t$). In addition, the range of the timestep difference is larger for a greater sampling timestep t , meaning that the slowed timestep at a greater timestep t is possibly more different from the sampling timestep t .

In light of the observation, we present a novel training method named MixFlow, which leverages the ground-truth noisy data at slowed timesteps, called slowed interpolation, for training the prediction network. The input noisy data to the prediction network at one training timestep is a mixture of slowed interpolations, containing the interpolation corresponding to the training timestep, as well as the interpolations at higher-noise timesteps. In our implementation, each slowed interpolation, is uniformly sampled for any training timestep, and the training timestep is sampled according to the probability Beta(2, 1). This implementation results in that each pair of slowed interpolation and training timestep, input to the prediction network, is uniformly sampled across all the pairs of slowed interpolation and training timestep. The implementation is very simple: only a few lines of code are modified for training with MixFlow. For example, only 5 lines are modified for MixFlow + RAE [54].

We demonstrate the effectiveness of MixFlow by post-training the generation models. Our approach outperforms representative methods that are developed for alleviating the training-testing discrepancy. Our approach consistently improves the performance on class-conditional image generation (such as SiT [26], REPA [52], and the very-recently developed method RAE [54]) and text-to-image generation. The MixFlow training approach over the RAE models achieve strong image generation results on ImageNet: 1.43 FID (without guidance) and 1.10 (with guidance) at 256×256 , and 1.55 FID (without guidance) and 1.10 (with guidance) at 512×512 .

2. Related Works

Visual generation with diffusion and flow. Flow [23–25, 30, 48] and diffusion models [9, 34, 35, 39, 40] have been widely applied for visual generation. Many variants have been presented. Prediction outputs include noise [9, 34], data [17], score [38–40], and velocity [23, 24]. Noise scheduling includes: variance preserving interpolation [40], and linear interpolation [23, 24]. Sampling algorithms include: DDIM [37], ODE [23], SDE [14], and so on. Other studies include backbone [3, 18, 26, 31, 34, 51], guidance mechanisms [8, 15] and latent representation [13, 19, 41,

44, 47, 49, 52, 54].

Alleviating exposure bias in diffusion and flow. The exposure bias issue is studied in diffusion models for visual generation. The techniques include new training schemes, e.g., Input Perturbation [27], and new inference schemes, e.g., Epsilon Scaling [28], Time-Shift Sampler [20], manifold constraint-based sampler [53] and multi-step denoising scheduled sampler [33].

Input Perturbation [27] trains the diffusion model by conducting a Gaussian perturbation on the ground truth noisy data to simulate the inference time prediction errors. The performance is sensitive to the perturbation strength: too large or too small even lead to worse result. Self Forcing [11], a novel training paradigm for autoregressive video diffusion models, uses previously-generated noisy data as the input for training diffusion models. As pointed out in Self Forcing [11], it is suitable for few-step diffusion as self forcing for standard many-step diffusion models would be computationally prohibitive.

Epsilon Scaling [28] adjusts the sampling process by scaling the noise prediction, mitigating the input mismatch between training and sampling. Time-Shift Sampler [20] modifies the sampling process by finding a coupled timestep of the previously sampled data, for the next sampling iteration. The coupled timestep ideally corresponds to the nearest ground truth noisy data, and is found heuristically in the sampling process. Differently, our approach addresses a related problem by modifying the training procedure.

3. Diffusion and Flow Matching

Flow matching and diffusion models adopt a stochastic process that transforms from the noise to the data. Usually, the noise distribution is a Gaussian distribution: $\mathbf{x}_0 \sim \mathcal{N}(0, 1)$, and the data distribution $\mathbf{x}_1 \sim q$ is represented by data samples. The interpolation, ground-truth noisy data, in the stochastic process can be formulated as a combination of the noise and the data:

$$\mathbf{x}_t = \alpha_t \mathbf{x}_1 + \beta_t \mathbf{x}_0, \quad (1)$$

where α_t increases when t increases and β_t decreases when t increases. Flow matching adopts the following setting:

$$\alpha_t = t, \quad \beta_t = 1 - t. \quad (2)$$

Variance-preserving diffusion models use $\alpha_t^2 + \beta_t^2 = 1$, e.g., generalized variance-preserving diffusion models [26] set:

$$\alpha_t = \sin\left(\frac{1}{2}\pi t\right), \quad \beta_t = \cos\left(\frac{1}{2}\pi t\right). \quad (3)$$

The model prediction output could be the noise, the data, the score, or the velocity. The loss function, using the velocity as the prediction target, is as follows,

$$\mathbb{E}_{t, \mathbf{x}_0, \mathbf{x}_1} [\|\mathbf{u}_\theta(\mathbf{x}_t, t) - \mathbf{u}^*(\mathbf{x}_t, t)\|_2^2], \quad (4)$$

where $\mathbf{u}^*(\mathbf{x}_t, t)$ is the ground truth velocity for the interpolation \mathbf{x}_t at the training timestep t .

The typical sampling algorithms include: reverse-time stochastic differential equation (SDE) sampler, $d\mathbf{x}_t = \mathbf{u}_\theta(\mathbf{x}_t, t)dt - \frac{1}{2}\bar{w}_t\mathbf{s}(\mathbf{x}_t, t)dt + \sqrt{\bar{w}_t}d\bar{\mathbf{w}}_t$, where \bar{w}_t is a reverse-time Wiener process, $\bar{w}_t > 0$ is an arbitrary time-dependent diffusion coefficient, $\mathbf{s}(\mathbf{x}_t, t)$ is the score; a probability flow ordinary differential equation (ODE) sampler, $d\mathbf{x}_t = \mathbf{u}_\theta(\mathbf{x}_t, t)dt$. The ODE can be numerically solved using the first-order Euler's method:

$$\mathbf{x}_{i+1} = \mathbf{x}_i + \Delta t \mathbf{u}_\theta(\mathbf{x}_i, t_i), \quad (5)$$

or the second-order Heun's method:

$$\begin{cases} \tilde{\mathbf{x}}_{i+1} = \mathbf{x}_i + \Delta t \mathbf{u}_\theta(\mathbf{x}_i, t_i) \\ \mathbf{x}_{i+1} = \mathbf{x}_i + \frac{\Delta t}{2} [\mathbf{u}_\theta(\mathbf{x}_i, t_i) + \mathbf{u}_\theta(\tilde{\mathbf{x}}_{i+1}, t_{i+1})], \end{cases} \quad (6)$$

where i is timestep index, and $\Delta t = t_{i+1} - t_i$ is step size.

4. MixFlow

The proposed MixFlow approach is inspired by the *Slow Flow* phenomenon shown in Figure 1. MixFlow includes several key points: slowed interpolation mixture for leveraging the ground truth noisy data from slowed timesteps, i.e., high-noise timesteps, for training the prediction network at each training timestep; loss function formulated with slowed interpolation mixture; as well as slowed timestep and training timestep sampling.

Slowed interpolation mixture. Standard diffusion and flow matching models adopt a *single* interpolation¹ \mathbf{x}_t at the training timestep t as input for training the prediction network, e.g., the velocity prediction network $\mathbf{u}_\theta(\mathbf{x}, t)$ in our study. Given the data \mathbf{x}_1 and the noise \mathbf{x}_0 , the interpolation is computed as Equation (1), and the interpolation coefficients α_t and β_t only correspond to the training timestep t .

Our approach, instead, uses an infinite mixture of interpolations as input for training $\mathbf{u}_\theta(\mathbf{x}, t)$ at the training timestep t :

$$\mathcal{X}_t = \{\mathbf{x}_{m_t} \mid \mathbf{x}_{m_t} = \beta_{m_t} \mathbf{x}_0 + \alpha_{m_t} \mathbf{x}_1, m_t \in \mathcal{M}_t\}, \quad (7)$$

where \mathcal{M}_t is the range of timesteps, relying on timestep t .

The timestep range \mathcal{M}_t is formed according to the *Slow Flow* phenomenon shown in Figure 1: The timestep corresponding to the ground truth interpolation that is nearest to the generated noisy data at the sampling timestep t is observed to be smaller than t , i.e., higher-noise timestep which we call *slowed timestep*; The slowed timestep range at greater sampling timestep t is larger, i.e., the slowed

¹In this paper, the two terms, interpolation and ground truth noisy data are about the same meaning without special description.

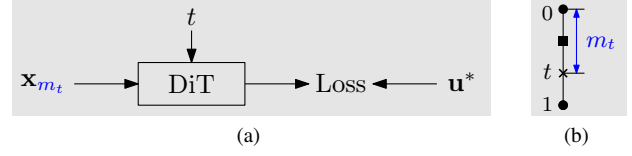


Figure 2. Illustrating MixFlow training. (a) MixFlow training. At the training timestep t , the input noisy data is the interpolation \mathbf{x}_{m_t} at the slowed timestep m_t . It is different from standard training: the input noisy data is the interpolation \mathbf{x}_t at the timestep t . (b) Slowed timestep. m_t is a timestep lying in the range $[(1 - \gamma)t, t]$. The illustration in (b) is for $\gamma = 1$.

timestep difference between the generated noisy data and the ground truth noisy data could be larger at greater sampling timestep.

We choose *slowed interpolation mixture*: a set of interpolations from a range of slowed timesteps:

$$\mathcal{M}_t = [(1 - \gamma)t, t]. \quad (8)$$

The mixture range size is: $t - (1 - \gamma)t = \gamma t$, which is linear with respect to the training timestep t . γ can be empirically selected or simply set as 1.

Loss function. Our approach with slowed interpolation mixture optimizes the following loss function,

$$\mathbb{E}_{t, \mathbf{x}_0, \mathbf{x}_1, m_t} [\|\mathbf{u}_\theta(\mathbf{x}_{m_t}, t) - \mathbf{u}^*(\mathbf{x}_t, t)\|_2^2]. \quad (9)$$

In comparison to the standard loss function in Equation (4), an extra variable, slowed timestep m_t , is introduced. The loss is not only about the interpolation at the training timestep t , but also the slowed interpolation \mathbf{x}_{m_t} at the higher-noise (slowed) timestep m_t .

The input noisy data to the prediction network \mathbf{u}_θ is the interpolation \mathbf{x}_{m_t} at a slowed timestep m_t instead of the interpolation \mathbf{x}_t at the training timestep t in standard training (Equation (4)). The input timestep is still the training timestep t (other than the slowed timestep m_t). It should be noted that the sampling process is the same with that for standard training and there is no need to compute slowed timestep m_t . Figure 2 illustrates of MixFlow training.

Training. The MixFlow loss function in Equation (9) introduces the extra variable m_t , the slowed timestep, which we need to handle for MixFlow training. We sample m_t at the training timestep t from a simple distribution $p(m_t|t)$, a uniform distribution:

$$m_t \sim \mathcal{U}[(1 - \gamma)t, t]. \quad (10)$$

The mixture range size of the slowed timesteps m_t at the training timestep t is γt . The conditional probability is thus $p(m_t|t) = \frac{1}{\gamma t}$ for $m_t \in [(1 - \gamma)t, t]$. We expect that all the pairs (\mathbf{x}_{m_t}, t) , the inputs to the prediction network \mathbf{u}_θ , are

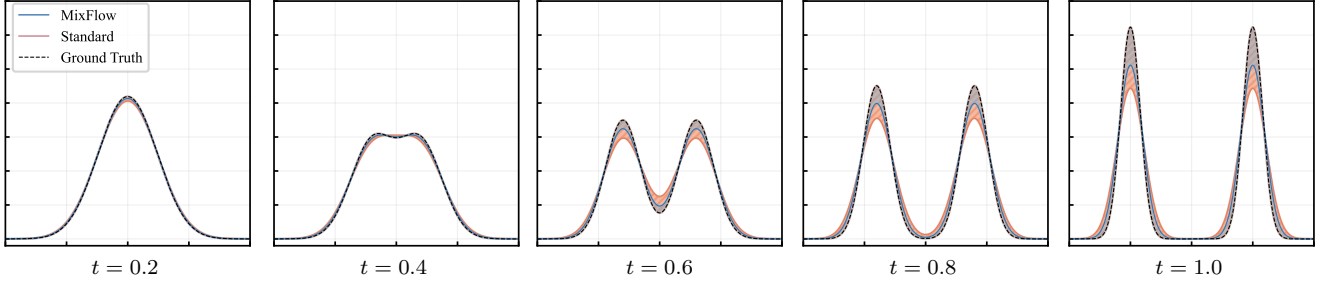


Figure 3. A toy example illustrating the advantage of the MixFlow training over the standard training. The distribution from the model with the MixFlow training fits better the ground truth distribution than the standard training. Details about this toy example are provided in Appendix B.

Algorithm 1 MixFlow Training

- 1: **Input:** dataset \mathcal{D} , initial model parameter θ , mixture range coefficient γ , learning rate η
- 2: **repeat**
- 3: Sample $\mathbf{x}_1 \sim \mathcal{D}$
- 4: Sample $\mathbf{x}_0 \sim \mathcal{N}(\mathbf{0}, \mathbf{I})$
- 5: Sample $t \sim \text{Beta}(2, 1)$
- 6: Sample $m_t \sim \mathcal{U}[(1 - \gamma)t, t]$
- 7: $\mathbf{x}_{m_t} \leftarrow \beta_{m_t} \mathbf{x}_0 + \alpha_{m_t} \mathbf{x}_1$
- 8: $\mathcal{L} \leftarrow \|\mathbf{u}_\theta(\mathbf{x}_{m_t}, t) - \mathbf{u}^*\|_2^2$
- 9: $\theta \leftarrow \theta - \eta \nabla_\theta \mathcal{L}$
- 10: **until** convergence

evenly sampled: $p(m_t, t) = p(m_{t'}, t')$. Considering that $p(m_t, t) = p(m_t|t)p(t)$, we have $p(t) \propto t$. Since $\int_0^1 p(t) = 1$ and $t \in [0, 1]$, $p(t) = 2t$, meaning that $p(t)$ is a Beta distribution

$$t \sim \text{Beta}(2, 1). \quad (11)$$

The algorithm is given in Algorithm 1. The key differences from standard training lie in Line 5 - Line 8.

Toy example. We use a 1D toy example to show that MixFlow training can generate samples that fit the data distribution better than standard training. The distribution for data x_1 is a mixture of two Gaussians: $p(x_1) = 0.5\mathcal{N}(x_1; -2, 0.1^2) + 0.5\mathcal{N}(x_1; 2, 0.1^2)$. The distribution for noise x_0 is a Gaussian: $p(x_0) = \mathcal{N}(x_0; 0, 1)$.

Figure 3 illustrates the distributions of generated noisy data at five sampling timesteps for MixFlow training, standard training, and ground truth. The observations include: MixFlow learns a better distribution than standard training; The discrepancy between the learned distribution and the ground truth distribution becomes larger at greater timesteps. The observations are consistent to Figure 1: MixFlow trains the model better; The timestep difference range, between the nearest ground truth data and the generated noisy data, becomes larger for larger sampling

timestep.

5. Experiments

5.1. Ablation Studies

We study key components in MixFlow over the SiT-B model [26]: sampling distributions for training timestep t and slowed timestep m_t , and mixture range coefficient γ . We implement the MixFlow training algorithm by modifying the official SiT implementation, and post-train the pre-trained model in $500K$ steps on ImageNet [1]. We use the same training hyperparameters, the same evaluation setting, the same ODE sampling process (second-order Heun sampler, 250 sampling steps) and the same classifier-free guidance scale (1.5) as the original setting in SiT [26]. The gFID score is used as the metric.

Sampling distributions for training timestep t and slowed timestep m_t . MixFlow samples the training timestep t from a Beta distribution $\text{Beta}(2, 1)$, and samples the slowed timestep m_t from a uniform distribution $\mathcal{U}[(1 - \gamma)t, t]$. In this study, we set mixture range coefficient γ as 1, i.e., $m_t \sim \mathcal{U}[0, t]$, and the choice of mixture range coefficient γ will be studied later. We study alternative sampling distributions: $t \sim \mathcal{U}[0, 1]$ and $m_t \sim \mathcal{U}[0, 1]$. Table 1 shows the study results.

Sampling the timestep m_t from $\mathcal{U}[0, t]$, i.e., only higher-noise timesteps can be sampled for interpolation mixture, yields better performance than sampling m_t from $\mathcal{U}[0, 1]$, i.e., both higher-noise and lower-noise timesteps can be sampled. The result for sampling m_t from $\mathcal{U}[0, 1]$, 18.27/5.07 and 18.25/5.06 is even worse than the result of the baseline model, 17.97/4.46. This indicates that the inclusion of the interpolations at lower-noise timesteps harms the training, i.e., harming in solving the *Slow Flow* problem.

In the case that $m_t \sim \mathcal{U}[0, t]$, sampling training timestep t from $\mathcal{U}[0, 1]$ performs better than the baseline: 16.58/4.25 vs 17.97/4.46 but worse than sampling t from $\text{Beta}(2, 1)$: 16.58/4.25 vs 15.64/3.93. This implies that evenly sampling the pair (m_t, t) benefits the training, which is consis-

Table 1. Studies of sampling distributions for t and m_t in the MixFlow training. The metric scores are for generation without guidance / generation with guidance.

	$t \sim \mathcal{U}[0, 1]$	$t \sim \text{Beta}(2, 1)$
$m_t \sim \mathcal{U}[0, 1]$	18.27 / 5.07	18.25 / 5.06
$m_t \sim \mathcal{U}[0, t]$	16.57 / 4.25	15.64 / 3.93

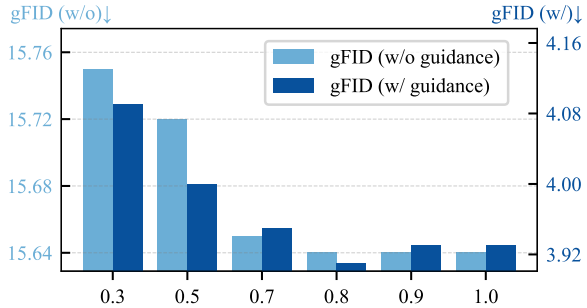


Figure 4. Studies of mixture range coefficient γ for sampling the slowed timestep: $m_t \sim \mathcal{U}[(1 - \gamma)t, t]$.

Table 2. Comparison of standard and MixFlow post-training.

	w/o guidance	w/ guidance
No post-training	17.97	4.46
Standard post-training	17.96	4.46
MixFlow post-training	15.64	3.91

tent to the analysis in Section 4.

Mixture range coefficient γ in the distribution $\mathcal{U}[(1 - \gamma)t, t]$ for sampling m_t . We consider seven values: $\{0.3, 0.5, 0.7, 0.8, 0.9, 1.0\}$. We do not show the results for $\gamma = 0$, which is slightly worse than baseline (18.00/4.48 vs 17.97/4.46). The results are given in Figure 4. $\gamma = 0.7, 0.8, 0.9, 1.0$ performs better and similarly. $\gamma = 0.8$ performs slightly better: the gFID scores without guidance for $\gamma = 0.7, 0.8, 0.9, 1.0$ are 15.65, 15.64, 15.64, 15.64 and the scores with guidance are 3.95, 3.91, 3.93, 3.93. The slightly-better performance might come from that the interpolations from the over-slowed timesteps e.g., $m_t \in [0, 0.2t]$, are not helpful as for the model from standard training at the sampling step t it is unlikely to be delayed to $[0, 0.2t]$, which is consistent to the observation as shown in Figure 1. We choose $\gamma = 0.8$ as the choice if not specified for the following experiments.

MixFlow training vs standard training. One may have a question: does the performance get improved if the same number of standard post-training steps are conducted. The results shown in Table 2 suggest that standard post-training almost does not affect the performance, and the gain from MixFlow post-training does not come from more training steps, but comes from the MixFlow training scheme.

5.2. Improvement by MixFlow Training

We validate the effectiveness of the MixFlow training by improvements over class-conditional generation and text-to-image generation models and comparison to methods to exposure bias alleviation.

Improvement over various class-conditional generation models. We post-train the prior SOTA class-conditional generation models that are from the officially-released models at GitHub, including SiT with linear and variance-preserving interpolations [26], REPA [52], and RAE [54]. We follow the training settings, including learning rate, batch size, which are used in the official implementation for each model. Without special description, the evaluation settings are the same: same sampling scheme (second-order Heun sampler), same guidance scale (1.5), and sample sampling steps (250).

SiT. We report the results on two model sizes: SiT-B (130M) and SiT-XL (675M). The results on ImageNet 256×256 are reported in Table 3. One can see that the overall performance of MixFlow is better across the two model sizes for generation without and with guidance. The gFID scores for generation with guidance are improved from 4.46 to 3.91 for SiT-B/2, and from 2.15 to 1.99 for SiT-XL/2.

We also report the results on ImageNet 512×512 over the SiT-XL model. The observation is consistent. MixFlow improves the performance, enhancing the gFID score without guidance from 9.72 to 7.99 and the gFID score with guidance from 2.71 to 2.53.

Table 4 shows the results for other sampling steps, $\{250, 50, 20\}$. One observation is that the gains from MixFlow become greater for fewer sampling steps. The reason is that the *Slow Flow* issue is more pronounced for fewer sampling steps, where the sampler approximation is coarser and the training and testing difference is larger.

SiT-diffusion. We report the results of a diffusion model, SiT with generalized variance-preserving interpolations (Equation (3)). Table 5 shows the results. The observations are consistent to flow matching that uses the linear interpolation in Equation (2): the overall performance gets improved for both generation without guidance and with guidance. The gFID scores are improved from 18.01 to 15.59 for generation without guidance, and from 4.55 to 4.35 for generation with guidance. This experiment demonstrates that MixFlow is applicable to diffusion models with variance preserving interpolations besides linear interpolations.

REPA. We demonstrate the effectiveness of MixFlow over the models that are trained with advanced schemes. We post-train the officially-released model trained with REPA. The post-training loss function consists of the alignment loss used in REPA [52] as well as the MixFlow loss. The evaluation schemes are the same as REPA [52], such as guidance scale (1.8) and guidance interval ($[0, 0.7]$).

Table 3. **The performance of MixFlow over two model scales: SiT-B and SiT-XL** for class-conditional generation on ImageNet.

Method	Generation w/o guidance					Generation w/ guidance				
	gFID ↓	sFID ↓	IS ↑	Pre. ↑	Rec. ↑	gFID ↓	sFID ↓	IS ↑	Pre. ↑	Rec. ↑
<i>ImageNet 256 × 256</i>										
SiT-B/2 + MixFlow	17.97 15.64	6.43 5.21	79.4 92.0	0.62 0.63	0.66 0.66	4.46 3.91	4.93 4.76	182.4 201.7	0.78 0.79	0.57 0.56
SiT-XL/2 + MixFlow	9.35 7.87	6.38 4.91	126.1 140.3	0.67 0.68	0.68 0.67	2.15 1.99	4.60 4.34	258.1 272.0	0.81 0.80	0.60 0.61
<i>ImageNet 512 × 512</i>										
SiT-XL/2 + MixFlow	9.72 7.99	7.50 6.53	119.1 131.0	0.78 0.79	0.64 0.64	2.71 2.53	4.25 4.21	239.1 246.2	0.83 0.84	0.54 0.54

Table 4. **The performance of MixFlow over various sampling steps:** 250, 50 and 20. The gain is more significant for fewer steps.

Method	gFID w/o guidance			gFID w/ guidance		
	250	50	20	250	50	20
<i>ImageNet 256 × 256</i>						
SiT-B/2	17.97	18.10	19.05	4.46	4.57	4.88
+ MixFlow	15.64	15.76	16.47	3.91	3.93	4.10
<i>Gain</i>	2.33	2.34	2.58	0.55	0.64	0.78
SiT-XL/2	9.35	9.73	10.67	2.15	2.17	2.28
+ MixFlow	7.87	8.00	8.71	1.99	2.01	2.09
<i>Gain</i>	1.48	1.73	1.96	0.16	0.16	0.19
<i>ImageNet 512 × 512</i>						
SiT-XL/2	9.72	11.12	13.50	2.71	2.83	3.12
+ MixFlow	7.99	9.01	10.82	2.53	2.59	2.84
<i>Gain</i>	1.73	2.11	2.68	0.18	0.24	0.28

The results are given in Table 5. Almost all the scores get improved except that the recall scores are the same. The gFID scores are improved: 6.90 → 6.28 for generation without guidance, and 1.65 → 1.59 for generation with guidance. The performance improvement indicates that MixFlow is compatible with the advanced training scheme, representation alignment.

RAE. We test the effectiveness of MixFlow over the very recently developed strong model trained with RAE [54] that is different from most existing methods and replaces the VAE with pretrained representation encoders (e.g., DINO [29]) paired with trained decoders. We post-train the officially-released model using MixFlow with $\gamma = 0.4$ for 200 epochs. The evaluation schemes are the same as RAE [54], such as sampling steps (50), auto-guidance and balanced sampling. The auto-guidance scale is 1.5.

The results are given in Table 5. One can see that the overall performance gets improved except that the IS scores are a little worse. The gFID scores are improved from 1.51 to 1.43 for generation without guidance and from 1.13 to 1.10 for generation with guidance [15]. The superior per-

formance shows that MixFlow is applicable to the scenario: learning diffusion models with the representation autoencoder paired with trained decoder, in addition to the widely-used VAE encoder and decoder.

Comparison to methods to exposure bias alleviation. We compare MixFlow against the modified training schemes, input perturbation [27], and the modified inference schemes, Epsilon Scaling [28], and Time-Shift sampler [20]. We implement these algorithms and do the post-training process with carefully hyperparameter tuning (details are provided in Appendix C) in the SiT code base.

Table 6 presents the comparison results. One can see that our approach MixFlow achieves the most significant improvement. The input perturbation algorithm may include the ground-truth noisy data at lower-noise timesteps for training. Such noisy data harms model training, which is validated in Section 5.1 and Table 1 ($m_t \sim \mathcal{U}[0, 1]$). Thus the perturbation strength needs to be well tuned. Otherwise, the performance gets worse.

The Time Shift sampler [20], a modified inference scheme, makes the timestep adjustment for the next step sampling. The timestep adjustment may not be accurate as the adjustment is heuristic, and the adjusted timestep may correspond to the higher-noise timestep, which implies that it often needs more sampling steps to reach the timestep 1. These are the reasons why this scheme gets worse results.

Epsilon Scaling sampling [28] is a method that moves the sampling trajectory closer to the vector field learned in the training phase by scaling the network output epsilon. One can see that it can improve the performance and it is inferior to our approach MixFlow. Similar to Time Shift, Epsilon Scaling is heuristic and the adjustment may not be accurate. The results indicate that our training approach, MixFlow, is advantageous.

Improvement over the text-to-image generation model SD 3.5. We demonstrate MixFlow on the text-to-image (T2I) generation task over the Stable Diffusion 3.5 model (SD 3.5-medium) [4]. We build a high-quality T2I dataset,

Table 5. The effectiveness of MixFlow on SiT with generalized variance-preserving interpolations, REPA and RAE.

Method	Generation w/o guidance					Generation w/ guidance				
	gFID ↓	sFID ↓	IS ↑	Pre. ↑	Rec. ↑	gFID ↓	sFID ↓	IS ↑	Pre. ↑	Rec. ↑
<i>Diffusion</i>										
SiT-B/2-GVP	18.01	6.38	79.39	0.61	0.66	4.55	4.91	181.60	0.78	0.56
+ MixFlow	15.59	6.31	90.52	0.63	0.64	4.35	4.88	199.94	0.79	0.54
<i>REPA</i>										
REPA-XL/2	6.90	6.03	148.9	0.68	0.69	1.65	4.63	278.3	0.77	0.65
+ MixFlow	6.28	5.06	159.8	0.69	0.69	1.59	4.34	290.5	0.78	0.65
<i>RAE</i>										
RAE-XL	1.51	5.31	242.9	0.79	0.63	1.13	4.74	262.6	0.78	0.67
+ MixFlow	1.43	4.81	239.8	0.80	0.64	1.10	4.40	259.7	0.78	0.67

Table 6. Comparison to representative methods to exposure bias alleviation. The results are based on SiT-B.

Method	Generation w/o guidance					Generation w/ guidance				
	gFID ↓	sFID ↓	IS ↑	Pre. ↑	Rec. ↑	gFID ↓	sFID ↓	IS ↑	Pre. ↑	Rec. ↑
SiT-B/2 [26]	17.97	6.43	79.4	0.62	0.66	4.46	4.93	182.4	0.78	0.57
+ Time-Shift [20]	18.12	6.41	79.5	0.62	0.66	4.49	4.80	180.5	0.78	0.56
+ Epsilon Scaling [28]	17.18	6.28	80.8	0.62	0.65	4.39	4.81	182.5	0.78	0.56
+ Input Perturbation [27]	17.01	5.37	83.1	0.62	0.65	4.32	4.77	185.8	0.78	0.56
+ MixFlow	15.64	5.21	92.0	0.63	0.66	3.91	4.76	201.7	0.79	0.56

Table 7. The performance for text-to-image generation.

Method	GenEval		DPG-Bench		T2I-CompBench		
	Avg. ↑	Counting ↑	Avg. ↑	Shape ↑	Spatial ↑	Complex ↑	
<i>40 sampling steps</i>							
SD 3.5	0.64	0.50	84.80	0.6555	0.2850	0.4202	
SD 3.5-ft-20k	0.64	0.51	84.90	0.6552	0.2852	0.4208	
SD 3.5-ft-10k	0.64	0.51	84.87	0.6556	0.2855	0.4205	
+ MixFlow	0.66	0.62	86.16	0.6912	0.3506	0.4556	
<i>10 sampling steps</i>							
SD 3.5	0.62	0.47	81.78	0.6344	0.2510	0.3872	
SD 3.5-ft-20k	0.62	0.48	81.83	0.6348	0.2532	0.3878	
SD 3.5-ft-10k	0.62	0.48	81.80	0.6349	0.2530	0.3874	
+ MixFlow	0.65	0.59	85.38	0.6809	0.3201	0.4165	

and finetune the model with the SD 3.5 training scheme for 10K steps, which is enough for convergence. We name the resulting model as SD 3.5-ft-10K. We post-train this model with the MixFlow training algorithm for 10K steps using the training hyperparameters same as SD 3.5. We build a baseline model, SD 3.5-ft-20K, by further post-training SD 3.5-ft-10K for extra 10K steps, to show that our superior results do not come from the extra training steps.

Table 7 gives the results over three metrics. The results for example sub-metrics are also included. Detailed results on more sub-metrics are in Appendix C and Table D.4. One

can see that the MixFlow training gets improved in terms of all the six metrics for both 40 and 10 sampling steps. The improvement shows that MixFlow is applicable to the text-to-image generation model, where the complex network structure MMDiT is used and the pretrained model is trained using advanced schemes.

Figure 5 shows visual results that demonstrate the advantage of MixFlow for three example sub-metrics: counting, spatial relation, and shape. The results are from 40 sampling steps. For example, from Figure 5 (b), one can see that our approach can follow the prompt to generate the image with a bird really on the left of a clock.

5.3. State-of-the-Art Class-Conditional Generation

We present the comparison with state-of-the-art models on ImageNet 256 × 256 and 512 × 512. We follow RAE [54] to use auto-guidance and class-balanced sampling for evaluation. The guidance scale is 1.5 for both 256 × 256 and 512 × 512, which is the same as RAE for 512 × 512.

Tables 8 and 9 present the results. The results without guidance for ImageNet 512 × 512 are included in Appendix E. MixFlow + RAE gets superior performance over all prior diffusion models in terms of gFID, setting new state-of-the-art gFID scores of 1.43 without guidance and 1.10 with guidance at 256 × 256, 1.55 without guidance and 1.10 with guidance at 512 × 512.

Our state-of-the-art FID score is supported by strong

Table 8. **Class-conditional performance on ImageNet** 256×256 . Our approach MixFlow achieves the best gFID score without guidance (1.43) and with guidance (1.10). We follow RAE [54] to use class-balanced sampling for some results, which are indicated in gray. The results for SiT, REPA, REPA + MixFlow and SiT+MixFlow are from the SDE sampler. The top 3 results per metric are marked in **bold**.

Method	Epochs	#Params	Generation w/o guidance					Generation w/ guidance				
			gFID \downarrow	sFID \downarrow	IS \uparrow	Prec. \uparrow	Rec. \uparrow	gFID \downarrow	sFID \downarrow	IS \uparrow	Prec. \uparrow	Rec. \uparrow
<i>Autoregressive</i>												
VAR [43]	350	2.0B	—	—	—	—	—	1.73	—	350.2	0.82	0.60
MAR [21]	800	943M	2.35	—	227.8	0.79	0.62	1.55	—	303.7	0.81	0.62
xAR [42]	800	1.1B	—	—	—	—	—	1.24	—	301.6	0.83	0.64
<i>Diffusion</i>												
ADM [2]	400	554M	10.94	6.02	101.0	0.69	0.63	3.94	6.14	215.8	0.83	0.53
RIN [12]	480	410M	3.42	—	182.0	—	—	—	—	—	—	—
PixNerd [45]	160	700M	—	—	—	—	—	1.87	4.36	298.0	0.79	0.61
SiD2 [10]	1280	—	—	—	—	—	—	1.38	—	—	—	—
DiT [31]	1400	675M	9.62	6.85	121.5	0.67	0.67	2.27	4.60	278.2	0.83	0.57
MaskDiT [55]	1600	675M	5.69	10.34	177.9	0.74	0.60	2.28	5.67	276.6	0.80	0.61
SiT [26]	1400	675M	8.61	6.32	131.7	0.68	0.67	2.06	4.50	270.3	0.82	0.59
MDTv2 [6]	1080	675M	—	—	—	—	—	1.58	4.52	314.7	0.79	0.65
REG [47]	800	677M	1.80	4.59	230.8	0.77	0.66	1.36	4.25	299.4	0.77	0.66
REPA [52]	800	675M	5.84	5.79	158.7	0.70	0.68	1.28	4.68	305.7	0.79	0.64
VA-VAE [49]	800	675M	2.05	4.37	207.7	0.77	0.66	1.25	4.15	295.3	0.80	0.65
REPA-E [19]	800	675M	1.69	4.17	219.3	0.77	0.66	1.12	4.09	302.9	0.79	0.66
DDT [46]	400	675M	6.27	—	154.7	0.68	0.69	1.26	—	310.6	0.79	0.65
RAE [54]	800	839M	1.51	5.31	242.9	0.79	0.63	1.13	4.74	262.6	0.78	0.67
MixFlow + SiT-XL	200	675M	7.56	4.75	144.5	0.69	0.68	1.97	4.34	276.8	0.82	0.60
MixFlow + REPA	200	675M	5.00	4.87	171.4	0.72	0.67	1.22	4.49	313.4	0.80	0.64
MixFlow + RAE	200	839M	1.43	4.81	239.8	0.80	0.64	1.10	4.40	259.7	0.78	0.67

Table 9. **Class-conditional performance on ImageNet** 512×512 with guidance.

Method	gFID \downarrow	sFID \downarrow	IS \uparrow	Prec. \uparrow	Rec. \uparrow
<i>Autoregressive</i>					
MAGViT-v2 [50]	1.91	—	324.3	—	—
VAR [43]	2.63	—	303.2	—	—
XAR [42]	1.70	—	281.5	—	—
<i>Diffusion</i>					
ADM [2]	3.85	5.86	221.7	0.84	0.53
SiD2 [10]	1.50	—	—	—	—
DiT [31]	3.04	5.02	240.8	0.84	0.54
EDM2 [16]	1.25	—	—	—	—
SiT [26]	2.62	4.18	252.2	0.84	0.57
DiffiT [7]	2.67	—	252.1	0.83	0.55
REPA [52]	2.08	4.19	274.6	0.83	0.58
REG [47]	1.68	3.87	306.9	0.80	0.63
DDT [46]	1.28	4.22	305.1	0.80	0.63
RAE [54]	1.13	4.24	259.6	0.80	0.63
MixFlow + RAE	1.10	4.17	256.9	0.80	0.65

qualitative results, which demonstrate high semantic diversity and fine-grained details. Visualization samples are provided in Appendix F.

6. Conclusion

We present a MixFlow training approach to alleviating exposure bias for diffusion models. The key is to exploit slowed interpolations, i.e., higher-noise interpolations, for training the prediction network at each training timestep. We demonstrate the effectiveness on various generation models. The MixFlow + RAE models achieve strong generation results on ImageNet: 1.43 FID (without guidance) and 1.10 (with guidance) at 256×256 , and 1.55 FID (without guidance) and 1.10 (with guidance) at 512×512 .

References

- [1] Jia Deng, Wei Dong, Richard Socher, Li-Jia Li, Kai Li, and Li Fei-Fei. Imagenet: A large-scale hierarchical image database. In *IEEE Conference on Computer Vision and Pattern Recognition (CVPR)*, 2009. 1, 4
- [2] Prafulla Dhariwal and Alexander Nichol. Diffusion models beat gans on image synthesis. *Neural Information Processing Systems (NeurIPS)*, 2021. 8
- [3] Patrick Esser, Sumith Kulal, Andreas Blattmann, Rahim Entezari, Jonas Müller, Harry Saini, Yam Levi, Dominik Lorenz, Axel Sauer, Frederic Boesel, et al. Scaling rectified flow transformers for high-resolution image synthesis. In *International Conference on Machine Learning (ICML)*, 2024. 2
- [4] Patrick Esser, Sumith Kulal, Andreas Blattmann, Rahim



Figure 5. Example results illustrating the advantages of MixFlow with respect to counting, spatial relationship and object shape. Left: SD 3.5; Middle: SD 3.5-ft-20k; Right: MixFlow.

Entezari, Jonas Müller, Harry Saini, Yam Levi, Dominik Lorenz, Axel Sauer, Frederic Boesel, et al. Scaling rectified flow transformers for high-resolution image synthesis. In *International Conference on Machine Learning (ICML)*, 2024. 6

[5] Kevin Frans, Danijar Hafner, Sergey Levine, and Pieter Abbeel. One step diffusion via shortcut models. In *The Thirteenth International Conference on Learning Representations, ICLR 2025, Singapore, April 24-28, 2025*, 2025. 14

[6] Shanghua Gao, Pan Zhou, Ming-Ming Cheng, and Shuicheng Yan. Mdtv2: Masked diffusion transformer is a strong image synthesizer. *arXiv preprint arXiv:2303.14389*, 2023. 8

[7] Ali Hatamizadeh, Jiaming Song, Guilin Liu, Jan Kautz, and Arash Vahdat. Diffit: Diffusion vision transformers for image generation. In *European Conference on Computer Vision (ECCV)*, 2024. 8

[8] Jonathan Ho and Tim Salimans. Classifier-free diffusion guidance. In *NeurIPS 2021 Workshop on Deep Generative Models and Downstream Applications*, 2021. 2

[9] Jonathan Ho, Ajay Jain, and Pieter Abbeel. Denoising diffusion probabilistic models. *Neural Information Processing Systems (NeurIPS)*, 2020. 2

[10] Emiel Hoogeboom, Thomas Mensink, Jonathan Heek, Kay Lamerigts, Ruiqi Gao, and Tim Salimans. Simpler diffusion (sid2): 1.5 fid on imagenet512 with pixel-space diffusion. *arXiv preprint arXiv:2410.19324*, 2024. 8

[11] Xun Huang, Zhengqi Li, Guande He, Mingyuan Zhou, and

Eli Shechtman. Self forcing: Bridging the train-test gap in autoregressive video diffusion. *Neural Information Processing Systems (NeurIPS)*, 2025. 1, 2

[12] Allan Jabri, David J. Fleet, and Ting Chen. Scalable adaptive computation for iterative generation. *International Conference on Machine Learning (ICML)*, 2023. 8

[13] Dengyang Jiang, Mengmeng Wang, Liuzhuozheng Li, Lei Zhang, Haoyu Wang, Wei Wei, Guang Dai, Yanning Zhang, and Jingdong Wang. No other representation component is needed: Diffusion transformers can provide representation guidance by themselves. *arXiv preprint arXiv:2505.02831*, 2025. 2

[14] Tero Karras, Miika Aittala, Timo Aila, and Samuli Laine. Elucidating the design space of diffusion-based generative models. *Neural Information Processing Systems (NeurIPS)*, 2022. 2

[15] Tero Karras, Miika Aittala, Tuomas Kynkänniemi, Jaakko Lehtinen, Timo Aila, and Samuli Laine. Guiding a diffusion model with a bad version of itself. In *Neural Information Processing Systems (NeurIPS)*, 2024. 2, 6

[16] Tero Karras, Miika Aittala, Jaakko Lehtinen, Janne Hellsten, Timo Aila, and Samuli Laine. Analyzing and improving the training dynamics of diffusion models. In *IEEE Conference on Computer Vision and Pattern Recognition (CVPR)*, 2024. 8, 16

[17] Diederik Kingma, Tim Salimans, Ben Poole, and Jonathan Ho. Variational diffusion models. *Neural Information Processing Systems (NeurIPS)*, 2021. 2

[18] Theodoros Kouzelis, Efstathios Karypidis, Ioannis Kakogiorgiou, Spyros Gidaris, and Nikos Komodakis. Boosting generative image modeling via joint image-feature synthesis. *arXiv preprint arXiv:2504.16064*, 2025. 2

[19] Xingjian Leng, Jaskirat Singh, Yunzhong Hou, Zhenchang Xing, Saining Xie, and Liang Zheng. Repa-e: Unlocking vae for end-to-end tuning of latent diffusion transformers. *IEEE International Conference on Computer Vision (ICCV)*, 2025. 2, 8

[20] Mingxiao Li, Tingyu Qu, Ruicong Yao, Wei Sun, and Marie-Francine Moens. Alleviating exposure bias in diffusion models through sampling with shifted time steps. *International Conference on Learning Representations (ICLR)*, 2024. 1, 2, 6, 7, 12

[21] Tianhong Li, Yonglong Tian, He Li, Mingyang Deng, and Kaiming He. Autoregressive image generation without vector quantization. *Neural Information Processing Systems (NeurIPS)*, 2024. 8

[22] Yangming Li and Mihaela van der Schaar. On error propagation of diffusion models. In *International Conference on Learning Representations (ICLR)*, 2024. 1

[23] Yaron Lipman, Ricky TQ Chen, Heli Ben-Hamu, Maximilian Nickel, and Matthew Le. Flow matching for generative modeling. In *International Conference on Learning Representations (ICLR)*, 2022. 2

[24] Xingchao Liu, Chengyue Gong, et al. Flow straight and fast: Learning to generate and transfer data with rectified flow. In *International Conference on Learning Representations (ICLR)*, 2023. 2

[25] Xingchao Liu, Xiwen Zhang, Jianzhu Ma, Jian Peng, et al. Instaflow: One step is enough for high-quality diffusion-based text-to-image generation. In *International Conference on Learning Representations (ICLR)*, 2023. 2

[26] Nanye Ma, Mark Goldstein, Michael S Albergo, Nicholas M Boffi, Eric Vanden-Eijnden, and Saining Xie. Sit: Exploring flow and diffusion-based generative models with scalable interpolant transformers. In *European Conference on Computer Vision (ECCV)*, 2024. 1, 2, 4, 5, 7, 8, 12, 16

[27] Mang Ning, Enver Sangineto, Angelo Porrello, Simone Calderara, and Rita Cucchiara. Input perturbation reduces exposure bias in diffusion models. In *International Conference on Machine Learning (ICML)*, 2023. 1, 2, 6, 7, 12

[28] Mang Ning, Mingxiao Li, Jianlin Su, Albert Ali Salah, and Itir Onal Ertugrul. Elucidating the exposure bias in diffusion models. *International Conference on Learning Representations (ICLR)*, 2024. 1, 2, 6, 7, 12

[29] Maxime Oquab, Timothée Darct, Théo Moutakanni, Huy V Vo, Marc Szafraniec, Vasil Khalidov, Pierre Fernandez, Daniel HAZIZA, Francisco Massa, Alaaeldin El-Nouby, et al. Dinov2: Learning robust visual features without supervision. *Transactions on Machine Learning Research (TMLR)*, 2024. 6

[30] George Papamakarios, Eric Nalisnick, Danilo Jimenez Rezende, Shakir Mohamed, and Balaji Lakshminarayanan. Normalizing flows for probabilistic modeling and inference. *Journal of Machine Learning Research*, 2021. 2

[31] William Peebles and Saining Xie. Scalable diffusion models with transformers. In *IEEE International Conference on Computer Vision (ICCV)*, 2023. 2, 8, 16

[32] Marc’Aurelio Ranzato, Sumit Chopra, Michael Auli, and Wojciech Zaremba. Sequence level training with recurrent neural networks. *arXiv preprint arXiv:1511.06732*, 2015. 1

[33] Zhiyao Ren, Yibing Zhan, Liang Ding, Gaoang Wang, Chaoyue Wang, Zhongyi Fan, and Dacheng Tao. Multi-step denoising scheduled sampling: Towards alleviating exposure bias for diffusion models. In *Proceedings of the AAAI Conference on Artificial Intelligence*, 2024. 1, 2

[34] Robin Rombach, Andreas Blattmann, Dominik Lorenz, Patrick Esser, and Björn Ommer. High-resolution image synthesis with latent diffusion models. In *IEEE Conference on Computer Vision and Pattern Recognition (CVPR)*, 2022. 2

[35] Chitwan Saharia, William Chan, Saurabh Saxena, Lala Li, Jay Whang, Emily L Denton, Kamyar Ghasemipour, Raphael Gontijo Lopes, Burcu Karagol Ayan, Tim Salimans, et al. Photorealistic text-to-image diffusion models with deep language understanding. *Neural Information Processing Systems (NeurIPS)*, 2022. 2

[36] Florian Schmidt. Generalization in generation: A closer look at exposure bias. *arXiv preprint arXiv:1910.00292*, 2019. 1

[37] Jiaming Song, Chenlin Meng, and Stefano Ermon. Denoising diffusion implicit models. In *International Conference on Learning Representations*. 2

[38] Kiwhan Song, Jaeyeon Kim, Sitan Chen, Yilun Du, Sham Kakade, and Vincent Sitzmann. Selective underfitting in diffusion models. *arXiv preprint arXiv:2510.01378*, 2025. 2

[39] Yang Song and Stefano Ermon. Generative modeling by estimating gradients of the data distribution. *Neural Information Processing Systems (NeurIPS)*, 2019. 2

[40] Yang Song, Jascha Sohl-Dickstein, Diederik P Kingma, Abhishek Kumar, Stefano Ermon, and Ben Poole. Score-based generative modeling through stochastic differential equations. In *International Conference on Learning Representations (ICLR)*, 2021. 2

[41] George Stoica, Vivek Ramanujan, Xiang Fan, Ali Farhadi, Ranjay Krishna, and Judy Hoffman. Contrastive flow matching. *arXiv preprint arXiv:2506.05350*, 2025. 2

[42] Ren Sucheng, Yu Qihang, He Ju, Shen Xiaohui, Yuille Alan, and Chen Liang-Chieh. Beyond next-token: Next-x prediction for autoregressive visual generation. *arXiv preprint arXiv:2502.20388*, 2025. 8

[43] Keyu Tian, Yi Jiang, Zehuan Yuan, Bingyue Peng, and Liwei Wang. Visual autoregressive modeling: Scalable image generation via next-scale prediction. *Neural Information Processing Systems (NeurIPS)*, 2024. 8

[44] Runqian Wang and Kaiming He. Diffuse and disperse: Image generation with representation regularization. *arXiv preprint arXiv:2506.09027*, 2025. 2

[45] Shuai Wang, Ziteng Gao, Chenhui Zhu, Weilin Huang, and Limin Wang. Pixnerd: Pixel neural field diffusion. *arXiv preprint arXiv:2507.23268*, 2025. 8

[46] Shuai Wang, Zhi Tian, Weilin Huang, and Limin Wang. Ddt: Decoupled diffusion transformer. *arXiv preprint arXiv:2504.05741*, 2025. 8

[47] Ge Wu, Shen Zhang, Ruijing Shi, Shanghua Gao, Zhenyuan Chen, Lei Wang, Zhaowei Chen, Hongcheng Gao, Yao Tang, Jian Yang, et al. Representation entanglement for generation: Training diffusion transformers is much easier than you think. *Neural Information Processing Systems (NeurIPS)*, 2025. 2, 8

[48] Yilun Xu, Ziming Liu, Max Tegmark, and Tommi Jaakkola. Poisson flow generative models. *Neural Information Processing Systems (NeurIPS)*, 2022. 2

[49] Jingfeng Yao, Bin Yang, and Xinggang Wang. Reconstruction vs. generation: Taming optimization dilemma in latent diffusion models. In *IEEE Conference on Computer Vision and Pattern Recognition (CVPR)*, 2025. 2, 8

[50] Lijun Yu, José Lezama, Nitesh B Gundavarapu, Luca Vervari, Kihyuk Sohn, David Minnen, Yong Cheng, Vighnesh Birodkar, Agrim Gupta, Xiuye Gu, et al. Language model beats diffusion–tokenizer is key to visual generation. *arXiv preprint arXiv:2310.05737*, 2023. 8, 16

[51] Qihang Yu, Mark Weber, Xueqing Deng, Xiaohui Shen, Daniel Cremers, and Liang-Chieh Chen. An image is worth 32 tokens for reconstruction and generation. *Neural Information Processing Systems (NeurIPS)*, 2024. 2

[52] Sihyun Yu, Sangkyung Kwak, Huiwon Jang, Jongheon Jeong, Jonathan Huang, Jinwoo Shin, and Saining Xie. Representation alignment for generation: Training diffusion transformers is easier than you think. In *International Conference on Learning Representations (ICLR)*, 2025. 2, 5, 8

[53] Yao Yuzhe, Chen Jun, Huang Zeyi, Lin Haonan, Wang Mengmeng, Guang Dai, and Wang Jingdong. Manifold con-

straint reduces exposure bias in accelerated diffusion sampling. *International Conference on Learning Representations (ICLR)*, 2024. [1](#), [2](#)

[54] Boyang Zheng, Nanye Ma, Shengbang Tong, and Saining Xie. Diffusion transformers with representation autoencoders. In *arXiv preprint arXiv:2510.11690*, 2025. [2](#), [5](#), [6](#), [7](#), [8](#), [16](#)

[55] Hongkai Zheng, Weili Nie, Arash Vahdat, and Anima Anandkumar. Fast training of diffusion models with masked transformers. *arXiv preprint arXiv:2306.09305*, 2023. [8](#)

A. Details for Figure 1

Implementation. The ground truth noisy data that is the nearest to the generated noisy data $\hat{\mathbf{x}}$ is the projected data of the generated noisy data along the velocity $\mathbf{x}_1 - \mathbf{x}_0$ for flow matching. The corresponding slowed timestep is computed as:

$$m_t = \frac{(\hat{\mathbf{x}}_t - \mathbf{x}_0)^\top (\mathbf{x}_1 - \mathbf{x}_0)}{\|\mathbf{x}_1 - \mathbf{x}_0\|_2^2}. \quad (12)$$

We perform the ODE sampling on 20,000 training images on the SiT-B model for 50 sampling steps from $t = 0.05$ to $t = 1.0$. For each sampling step t , we collect the slowed timesteps m_t across all 20,000 images. The shaded area represents the range of slowed timesteps at each sampling timestep. At each sampling timestep, the lower point is the minimum slowed timestep, and the upper point is the maximum slowed timestep among all the 20,000 images.

Slow Flow for diffusion with GVP. Figure A.1 shows the Slow Flow phenomenon for diffusion with generalized variance preserving interpolations the on SiT-B model [26]. Different from flow matching that uses linear interpolation, we find the nearest ground truth noisy data by checking 1000 noisy data samples for each generated noisy data and record the corresponding slowed timestep. The observation is consistent to that for flow matching in Figure 1 in the main paper.

B. Details for Figure 3

The distribution for noise x_0 is a Gaussian: $p(x_0) = \mathcal{N}(x_0; 0, 1)$. The distribution for data x_1 is a mixture of two Gaussians: $p(x_1) = 0.5\mathcal{N}(x_1; -2, 0.1^2) + 0.5\mathcal{N}(x_1; 2, 0.1^2)$.

The velocity prediction network is an MLP with 4 hidden layers, 256 hidden dimensions, and the Swish activation function. The optimizer is Adam with learning rate 0.001. The batch size is 2,048. The training iteration number is 26,000 for standard training, and 6,000 from the model trained with 20,000 iterations for MixFlow training.

We use the Euler method with 5 sampling steps. We transform the generated noisy data to a distribution, by using Kernel Density Estimation (KDE) as implemented in the SciPy library. We utilize the default hyperparameter configuration: employ a Gaussian kernel with the bandwidth determined via Scott's Rule.

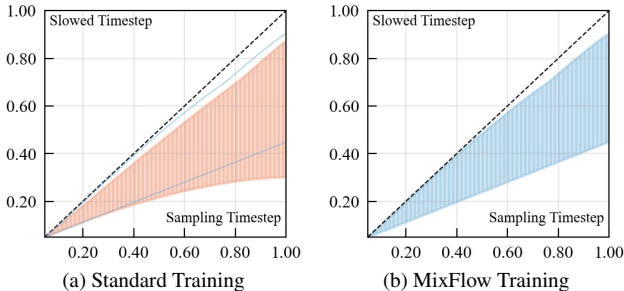


Figure A.1. **Slow Flow for diffusion models.** The upper and lower envelopes of the shading area in (b) are shown in (a).

C. More Results for Ablation Studies (Section 5.1)

We present more results in terms of other metrics for ablation studies.

Sampling distributions for t and m_t . Table C.2 presents the results for other metrics, including sFID, IS, Precision, and Recall. The overall observations are consistent to that for the gFID metric.

Mixture range coefficient γ in the distribution $\mathcal{U}[(1 - \gamma)t, t]$ for sampling m_t . Table C.3 presents the results for sFID, IS, Precision, and Recall for $\gamma \in \{0.0, 0.3, 0.5, 0.7, 0.8, 0.9, 1.0\}$. The observations are also consistent to that for the gFID metric.

D. More Results for Improvement by MixFlow Training (Section 5.2)

Results for SDE sampling. We present the results for SDE samplers [26] in Table C.1. The evaluation settings are the same: same guidance scale (1.5), and same sampling steps (250). The sampling scheme is first-order Euler-Maruyama integrator. The observations are the same for the ODE sampler.

Input Perturbation [27]. Input Perturbation trains the diffusion model by conducting a Gaussian perturbation on the ground truth noisy data to simulate the inference time prediction errors. We implement the input perturbation algorithm by carefully tuning the perturbation strength.

Table D.1 studies the effect of perturbation strengths. The performance is sensitive to the perturbation strength: too large or too small lead to poor result. In the main paper, we report the best one for strength 0.15.

Time Shift sampler [20]. Time-Shift Sampler modifies the sampling process by adjusting the timestep for the next sampling iteration based on the previously sampled data. Table D.3 presents the results on how the two hyperparameters, window size and cutoff value, affect the performance. We report the best result in the main paper.

Epsilon Scaling sampler [28]. Epsilon Scaling adjusts the sampling process by scaling the noise prediction, mitigating the input mismatch between training and sampling. It moves the sampling trajectory closer to the vector field learned in the training phase by scaling the network output epsilon.

Table D.2 studies the effect of scaling strength $\lambda(t) = kt + b$. The performance is sensitive to the choice of (k, b) . We report the best result in the main paper.

Text-to-image generation. We present the results for the submetrics from GenEval and T2I-CompBench. Table D.4 shows the results for T2I-CompBench across six attributes: Color, Shape, Texture, Spatial, Non-Spatial, and Complex. Table D.5 shows the results for GenEval across six categories: Single Object, Two Objects, Counting, Colors, Position, and Attribute Binding. MixFlow consistently improves the performance across all the metrics.

RAE. Figure D.1 presents the slow flow phenomenon that is observed in the RAE models. The overall observation is similar: MixFlow training makes slowed timesteps be closer to sampling timesteps, and the range for slowed timesteps be smaller. One difference from Figure 1 in the main paper and Figure A.1 is that the

Table C.1. **The performance with the SDE sampler** for class-conditional generation on ImageNet 256×256 and 512×512 .

Method	Generation w/o guidance					Generation w/ guidance				
	gFID \downarrow	sFID \downarrow	IS \uparrow	Pre. \uparrow	Rec. \uparrow	gFID \downarrow	sFID \downarrow	IS \uparrow	Pre. \uparrow	Rec. \uparrow
<i>ImageNet 256 \times 256</i>										
SiT-B/2 + MixFlow	17.19 14.47	6.51 5.23	82.9 96.3	0.63 0.65	0.66 0.65	4.10 3.74	4.98 4.52	192.4 212.5	0.79 0.80	0.56 0.54
SiT-XL/2 + MixFlow	8.26 7.56	6.32 4.75	131.7 144.5	0.68 0.69	0.67 0.67	2.06 1.97	4.60 4.34	270.3 276.8	0.83 0.82	0.59 0.60
<i>ImageNet 512 \times 512</i>										
SiT-XL/2 + MixFlow	9.20 8.46	7.33 5.76	125.3 139.7	0.78 0.79	0.64 0.64	2.62 2.49	4.18 4.01	252.2 268.9	0.84 0.84	0.57 0.57

Table C.2. **Studies of sampling distributions for t and m_t in the MixFlow training.**

	Generation w/o guidance					Generation w/ guidance				
	gFID \downarrow	sFID \downarrow	IS \uparrow	Pre. \uparrow	Rec. \uparrow	gFID \downarrow	sFID \downarrow	IS \uparrow	Pre. \uparrow	Rec. \uparrow
$m_t \sim \mathcal{U}[0, t], t \sim \mathcal{U}[0, 1]$	16.57	5.30	88.4	0.62	0.64	4.25	4.77	195.9	0.78	0.55
$m_t \sim \mathcal{U}[0, 1], t \sim \mathcal{U}[0, 1]$	18.27	5.74	75.8	0.62	0.66	5.07	4.89	168.9	0.77	0.56
$m_t \sim \mathcal{U}[0, t], t \sim \text{Beta}(2, 1)$	15.64	5.31	90.5	0.63	0.64	3.93	4.74	201.8	0.78	0.55
$m_t \sim \mathcal{U}[0, 1], t \sim \text{Beta}(2, 1)$	18.25	5.73	76.3	0.62	0.65	5.06	4.88	168.8	0.77	0.57

Table C.3. **Studies of sampling distributions of m_t . $m_t \sim \mathcal{U}[(1 - \gamma)t, t]$.**

	Generation w/o guidance					Generation w/ guidance				
	gFID \downarrow	sFID \downarrow	IS \uparrow	Pre. \uparrow	Rec. \uparrow	gFID \downarrow	sFID \downarrow	IS \uparrow	Pre. \uparrow	Rec. \uparrow
SiT-B/2	17.97	6.43	79.4	0.62	0.66	4.46	4.93	182.4	0.78	0.57
$\gamma = 0.0$	18.00	6.45	79.1	0.62	0.66	4.48	5.01	181.1	0.78	0.57
$\gamma = 0.3$	15.75	5.28	84.1	0.63	0.65	4.09	5.04	195.7	0.79	0.56
$\gamma = 0.5$	15.72	5.20	87.8	0.63	0.65	4.00	4.80	197.2	0.79	0.56
$\gamma = 0.7$	15.65	5.22	90.2	0.63	0.66	3.95	4.76	200.6	0.79	0.56
$\gamma = 0.8$	15.64	5.21	92.0	0.63	0.66	3.91	4.76	201.7	0.79	0.56
$\gamma = 0.9$	15.64	5.24	91.0	0.63	0.66	3.93	4.71	201.6	0.79	0.56
$\gamma = 1.0$	15.64	5.31	90.5	0.63	0.64	3.93	4.74	201.8	0.78	0.55

Table D.1. **The effect of perturbation strength in DDPM-IP.** The performance is sensitive to perturbation strength.

Strength	Generation w/o guidance					Generation w/ guidance				
	gFID \downarrow	sFID \downarrow	IS \uparrow	Pre. \uparrow	Rec. \uparrow	gFID \downarrow	sFID \downarrow	IS \uparrow	Pre. \uparrow	Rec. \uparrow
0.1	17.26	5.82	81.8	0.62	0.66	4.36	4.73	183.9	0.78	0.57
0.15	17.01	5.37	83.1	0.62	0.65	4.32	4.77	185.8	0.78	0.56
0.2	17.55	6.44	81.1	0.62	0.65	4.86	6.56	180.3	0.78	0.55
0.3	17.82	8.45	80.2	0.62	0.62	5.41	9.08	178.9	0.78	0.53
0.5	33.50	61.8	51.5	0.50	0.55	14.46	47.4	125.4	0.68	0.44

minimum slowed timestep is larger. For example, in Figure D.1 (a), the minimum slowed timestep around sampling timestep 1.00 is about 0.6, larger than 0.2 in Figure 1 in the main paper. This implies that the slowed timestep for RAE is possible to be closer to the sampling timestep.

Regarding the mixture range coefficient γ , we tried two choices: 0.8 that is selected for all the other experiments, and 0.4 ($= 1.00 - 0.60$) that is based on the observation in Figure D.1.

Both achieve similar performance (See Table D.6 and Figure D.1). $\gamma = 0.8$ needs 430 training epochs and $\gamma = 0.4$ needs around a half, 200, training epochs. Figure D.1 (d) shows that the upper and lower envelopes of slowed timesteps for $\gamma = 0.4$ and $\gamma = 0.8$ are almost the same. In the main paper, we report the results for $\gamma = 0.4$.

We additionally report the performance of RAE with 20 sampling steps in Table D.7. One can see that the improvement from

Table D.2. **The effect of scaling strength** $\lambda(t) = kt + b$ **in Epsilon Scaling.** The performance is sensitive to scaling strength.

	Generation w/o guidance					Generation w/ guidance				
	gFID ↓	sFID ↓	IS ↑	Pre. ↑	Rec. ↑	gFID ↓	sFID ↓	IS ↑	Pre. ↑	Rec. ↑
$k = 0, b = 1.02$	18.13	6.55	78.1	0.60	0.65	4.78	5.12	179.1	0.77	0.57
$k = 0, b = 1.015$	17.87	6.41	79.1	0.62	0.66	4.49	4.94	181.6	0.78	0.56
$k = 0, b = 1.01$	17.47	6.27	79.6	0.62	0.66	4.46	4.90	182.0	0.78	0.56
$k = 0, b = 1.005$	17.28	6.28	80.3	0.62	0.66	4.40	4.80	182.4	0.78	0.56
$k = 0, b = 0.995$	18.19	6.55	77.9	0.61	0.65	4.87	5.22	178.1	0.77	0.57
$k = 0, b = 0.99$	18.87	6.87	75.01	0.60	0.65	5.07	5.43	175.1	0.77	0.57
$k = 0.0001, b = 1.005$	17.18	6.28	80.8	0.62	0.65	4.39	4.81	182.5	0.78	0.56
$k = 0.0002, b = 1.005$	17.25	6.31	80.1	0.62	0.65	4.42	4.91	182.1	0.78	0.56
$k = 0.0004, b = 1.005$	17.51	6.30	79.1	0.62	0.64	4.47	4.97	179.1	0.78	0.56

MixFlow is larger than that for 50 sampling steps.

E. SOTA Results on ImageNet 512 × 512 without Guidance.

We present the comparison with state-of-the-art models on ImageNet 512 × 512 for generation without guidance in Table D.8. We compare with the methods that have reported performance on ImageNet 512 × 512 without guidance. We follow the same evaluation setting as in the main paper. MixFlow + RAE achieves the best performance across multiple metrics, including gFID, sFID, IS and Precision.

F. Qualitative Results

Class-conditional generation on ImageNet 256 × 256 and 512 × 512. We present the visualization results for MixFlow + RAE class-conditional generation on ImageNet 256 × 256 and 512 × 512 in Figures H.1 to H.12. The results demonstrate high semantic diversity and fine details.

G. Example Code

The MixFlow training implementation is very simple. For example, only **5 lines** of code are modified for the RAE implementation. The modification example is shown in Figure H.13.

H. Extensions

The initial results show that the MixFlow training algorithm also benefit (1) training the SiT model from scratch and training the shortcut model [5] for few-step sampling.

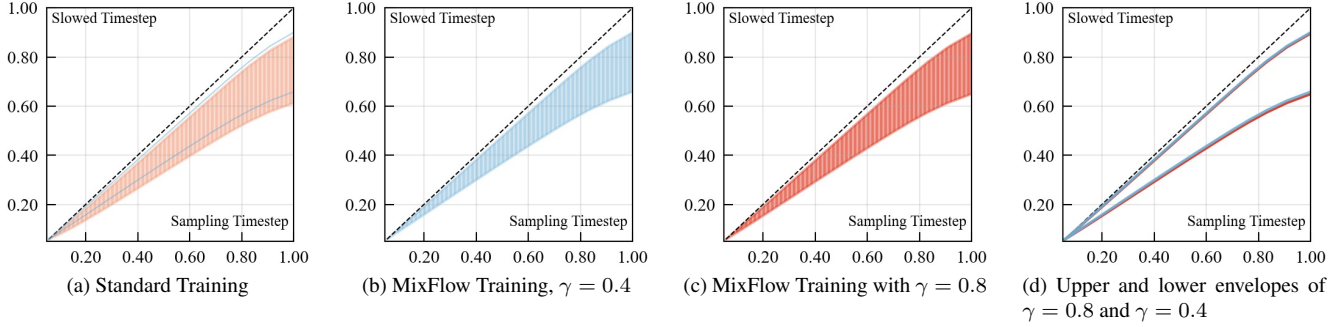


Figure D.1. Slow Flow for the RAE model.

Table D.3. The effect of window size and cutoff value in Time-Shift Sampler.

	Generation w/o guidance					Generation w/ guidance				
	gFID ↓	sFID ↓	IS ↑	Pre. ↑	Rec. ↑	gFID ↓	sFID ↓	IS ↑	Pre. ↑	Rec. ↑
w = 5, cutoff = 500	18.24	6.57	78.1	0.61	0.66	4.54	4.89	177.1	0.77	0.56
w = 5, cutoff = 400	18.20	6.50	78.3	0.61	0.66	4.54	4.89	178.4	0.77	0.56
w = 5, cutoff = 300	18.17	6.48	79.1	0.62	0.66	4.52	4.87	179.2	0.78	0.56
w = 5, cutoff = 200	18.14	6.44	79.5	0.62	0.66	4.50	4.82	180.9	0.78	0.56
w = 5, cutoff = 100	18.13	6.43	79.9	0.62	0.66	4.49	4.82	181.7	0.78	0.56
w = 5, cutoff = 50	18.15	6.45	79.1	0.62	0.66	4.50	4.82	180.9	0.78	0.56
w = 2, cutoff = 100	18.13	6.40	80.1	0.62	0.66	4.49	4.90	181.2	0.78	0.56
w = 8, cutoff = 100	18.12	6.41	79.5	0.62	0.66	4.49	4.80	180.5	0.78	0.56
w = 10, cutoff = 100	18.14	6.44	79.1	0.62	0.66	4.50	4.80	180.3	0.78	0.56

Table D.4. The performance for text-to-image generation in T2I-CompBench.

Method	Color ↑	Shape ↑	Texture ↑	Spatial ↑	Non-Spatial ↑	Complex ↑
SD 3.5	0.8135	0.6555	0.7841	0.2850	0.3129	0.4202
SD 3.5-ft-20k	0.8142	0.6556	0.7842	0.2852	0.3133	0.4208
SD 3.5-ft-10k	0.8140	0.6556	0.7839	0.2855	0.3132	0.4205
+ MixFlow	0.8507	0.6912	0.8009	0.3506	0.3381	0.4556

Table D.5. The performance for text-to-image generation in Geneval.

Method	Single Obj.	Two Obj.	Counting	Colors	Position	Attr. Bind.
SD 3.5	0.98	0.78	0.50	0.81	0.24	0.52
SD 3.5-ft-20k	0.98	0.78	0.51	0.80	0.24	0.52
SD 3.5-ft-10k	0.98	0.78	0.51	0.80	0.24	0.51
+ MixFlow	0.98	0.78	0.62	0.81	0.27	0.54

Table D.6. The effect of mixture range coefficient γ for RAE.

γ	Epochs	Generation w/o guidance					Generation w/ guidance				
		gFID \downarrow	sFID \downarrow	IS \uparrow	Pre. \uparrow	Rec. \uparrow	gFID \downarrow	sFID \downarrow	IS \uparrow	Pre. \uparrow	Rec. \uparrow
0.4	200	1.43	4.81	239.8	0.80	0.64	1.10	4.40	259.7	0.78	0.67
0.8	200	1.57	4.95	233.5	0.80	0.63	1.21	4.60	248.9	0.78	0.65
0.8	430	1.43	4.85	239.1	0.80	0.64	1.10	4.42	259.3	0.78	0.66

Table D.7. MixFlow on RAE. The gain for 20 sampling steps is larger than 50 sampling steps.

Method	Generation w/o guidance					Generation w/ guidance				
	gFID \downarrow	sFID \downarrow	IS \uparrow	Pre. \uparrow	Rec. \uparrow	gFID \downarrow	sFID \downarrow	IS \uparrow	Pre. \uparrow	Rec. \uparrow
<i>50 sampling steps</i>										
RAE	1.51	5.31	242.9	0.79	0.63	1.13	4.74	262.6	0.78	0.67
+ MixFlow	1.43	4.81	239.8	0.80	0.64	1.10	4.40	259.7	0.78	0.67
<i>20 sampling steps</i>										
RAE	1.92	6.32	232.8	0.78	0.64	1.35	5.37	254.4	0.77	0.67
+ MixFlow	1.64	5.39	238.7	0.80	0.63	1.18	4.77	255.8	0.78	0.66

Table D.8. Class-conditional performance on ImageNet 512 \times 512 without guidance.

Method	gFID \downarrow	sFID \downarrow	IS \uparrow	Prec. \uparrow	Rec. \uparrow
<i>Autoregressive</i>					
MAGViT-v2 [50]	3.07	–	213.1	–	–
<i>Diffusion</i>					
DiT [31]	11.93	–	–	–	–
SiT [26]	9.20	7.33	125.3	0.78	0.64
EDM2 [16]	1.91	–	–	–	–
RAE [54]	1.61	4.96	234.1	0.81	0.63
MixFlow + RAE	1.55	4.67	237.0	0.82	0.60



Figure H.1. **Uncurated** 256×256 MixFlow-XL samples.
AutoGuidance Scale = 1.5
Class label = “Sulphur-crested cockatoo” (89)



Figure H.2. **Uncurated** 256×256 MixFlow-XL samples.
AutoGuidance Scale = 1.5
Class label = “golden retriever” (207)



Figure H.3. **Uncurated 256×256 MixFlow-XL samples.**
 AutoGuidance Scale = 1.5
 Class label = “husky” (250)



Figure H.4. **Uncurated 256×256 MixFlow-XL samples.**
 AutoGuidance Scale = 1.5
 Class label = “arctic wolf” (270)



Figure H.5. **Uncurated** 256×256 MixFlow-XL samples.
AutoGuidance Scale = 1.5
Class label = “panda” (388)



Figure H.6. **Uncurated** 256×256 MixFlow-XL samples.
AutoGuidance Scale = 1.5
Class label = “balloon” (417)



Figure H.7. **Uncurated** 512×512 MixFlow-XL samples.
AutoGuidance Scale = 1.5
Class label = “Loggerhead sea turtle” (33)



Figure H.8. **Uncurated** 512×512 MixFlow-XL samples.
AutoGuidance Scale = 1.5
Class label = “macaw” (88)



Figure H.9. **Uncurated** 512×512 MixFlow-XL samples.
AutoGuidance Scale = 1.5
Class label = “lion” (291)



Figure H.10. **Uncurated** 512×512 MixFlow-XL samples.
AutoGuidance Scale = 1.5
Class label = “red panda” (387)



Figure H.11. **Uncurated** 512×512 MixFlow-XL samples.
AutoGuidance Scale = 1.5
Class label = “ice cream” (928)



Figure H.12. **Uncurated** 512×512 MixFlow-XL samples.
AutoGuidance Scale = 1.5
Class label = “coral reef” (973)

(a) RAE: Uniform sampling for the training timestep

```

def sample(self, x1):
    """Sampling x0 & t based on shape of x1 (if
    needed)
    Args:
        x1 - data point; [batch, *dim]
    """

    x0 = th.randn_like(x1)
    dist_options = self.time_dist_type.split("_")
    t0, t1 = self.check_interval(self.train_eps,
        self.sample_eps)
    if dist_options[0] == "uniform":
        t = th.rand((x1.shape[0],)) * (t1 - t0) +
        t0
    # ...

    t = t.to(x1)
    t = self.time_dist_shift * t / (1 + (self.
        time_dist_shift - 1) * t)
    return t, x0, x1

```

(c) RAE: Standard training loss

```

def training_losses(self, model, x1,
    model_kwargs=None):
    """Loss for training the score model
    Args:
        - model: backbone model; could be score,
        noise, or velocity
        - x1: datapoint
        - model_kwargs: additional arguments for the
        model
    """
    if model_kwargs == None:
        model_kwargs = {}

    t, x0, x1 = self.sample(x1)

    t, xt, ut = self.path_sampler.plan(t, x0, x1)

    model_output = model(xt, t, **model_kwargs)
    B, *_ , C = xt.shape
    assert model_output.size() == (B, *xt.size()
        [1:-1], C)

    terms = {}
    terms['pred'] = model_output
    if self.model_type == ModelType.VELOCITY:
        terms['loss'] = mean_flat(((model_output
        - ut) ** 2))
    else:
        # ...

    return terms

```

(b) MixFlow: Beta sampling for the training timestep

```

def sample(self, x1):
    """Sampling x0 & t based on shape of x1 (if
    needed)
    Args:
        x1 - data point; [batch, *dim]
    """

    x0 = th.randn_like(x1)
    dist_options = self.time_dist_type.split("_")
    t0, t1 = self.check_interval(self.train_eps,
        self.sample_eps)
    if dist_options[0] == "uniform":
        t = th.rand((x1.shape[0],)) * (t1 - t0) +
        t0
    # ...
    # Sample t from Beta(2,1)
    t = 1 - th.sqrt(1 - t)
    t = t.to(x1)
    t = self.time_dist_shift * t / (1 + (self.
        time_dist_shift - 1) * t)
    return t, x0, x1

```

(d) MixFlow: Training loss with mixed slowed interpolations

```

def training_losses(self, model, x1, gamma=0.4,
    model_kwargs=None):
    """Loss for training the score model
    Args:
        - model: backbone model; could be score,
        noise, or velocity
        - x1: datapoint
        - model_kwargs: additional arguments for the
        model
    """
    if model_kwargs == None:
        model_kwargs = {}

    t, x0, x1 = self.sample(x1)
    # Remove the standard interpolated xt
    t, _, ut = self.path_sampler.plan(t, x0, x1)
    # Sample slowed timestep mt
    mt = t + th.rand_like(t) * gamma * (1 - t)
    # Compute slowed interpolation
    _, xt, __ = self.path_sampler.plan(mt, x0, x1)
    model_output = model(xt, t, **model_kwargs)
    B, *_ , C = xt.shape
    assert model_output.size() == (B, *xt.size()
        [1:-1], C)

    terms = {}
    terms['pred'] = model_output
    if self.model_type == ModelType.VELOCITY:
        terms['loss'] = mean_flat(((model_output
        - ut) ** 2))
    else:
        # ...

    return terms

```

Figure H.13. **Only 5 lines of code are modified.** for the RAE implementation. Two functions in <https://github.com/bytetriper/RAE/blob/main/src/stage2/transport/transport.py> are modified. Left: RAE; Right: MixFlow + RAE. Note: in the RAE implementation, $t = 1$ corresponds to the noise and $t = 0$ corresponds to the clean data. The lines corresponds to the modified code.